Characterization Techniques for the Study of Silica Fragmentation in the Early Stages of Ethylene Polymerization

Walter D. Niegisch,* Salvatore T. Crisafulli, Tatyana S. Nagel, and Burkhard E. Wagner*

Union Carbide Chemicals and Plastics Company, Inc., P.O. Box 670, Bound Brook, New Jersey 08805

Received February 9, 1992

ABSTRACT: Cryomicrotomy of embedded particles, sequential removal of polymeric components via carefully controlled plasma ashing, and a combination of these preparative techniques allowed the microscopic characterization of the internal morphology and chemical composition of inorganic supports, supported catalysts, growing and fully grown polymer particles, and extruded films at submicrometer resolution. Videotaped polymerizations under a microscope at commercially used pressures provided additional insights into the particle growth process. The basic morphological units of polymer growth in olefin polymerization-grade silicas such as Davison 952 appear to be the intermediate, microspheroidal aggregates of 0.05–0.1 μm diameter. Polymerization initially causes replication of these nodules. The support lattice cracks within the first filling of the pore structure, but the dispersal of the resultant fragments into the submicrometer residues observed in the fully grown polymer particle (15-fold growth) is a more gradual process which is not yet completed after a 5-fold growth of the particle.

I. Introduction

Despite the world-wide commercial use of silica-supported catalysts for over 30 years,[1] the changes occurring in the support during and after the initiation of polymerization are not well understood. The fate of the silica carrier during polymerization is difficult to follow since the fragmented carrier remains embedded in the nascent polymer particle. Removal of the polymer component tends to change the size, shape, size distribution, and location of the residual carrier. In this paper we describe the use of several preparative and analytical techniques for the characterization of the silica carrier in the catalyst and the silica residues in nascent polymer particles and in extruded film. Our studies have allowed us to obtain a clearer understanding of the role and the fate of the carrier during ethylene polymerization with chromium oxide[1,2] or chromocene[3] catalysts supported on silica. The techniques appear to be equally applicable to other supports and catalysts.

Published work[2] has centered on the industrially important support Davison 952, which has a pore volume of ca. 1.5 cm^3/g, a 20-nm average pore diameter, and a surface area of ca. 300 m^2/g. The support consists of multilevel aggregates of 10–50-nm-diameter primary silica particles. Active sites for polymerization consist of transition-metal complexes distributed uniformly within the support. Polymerization at commercial yields then produces ca. 3000–10 000 g of polymer/g of silica, where the support remains embedded within the generated polymer particles.

McDaniel was the first to investigate the silica fragmentation process.[4] He addressed the need for careful isolation of the residual silica by ashing polymer particles in a furnace at 650 °C and attempted to disperse the resulting fused inorganic aggregates via agitation in an ultrasonic cleaner. This study suggested that the shattering process is independent of both the chemical nature of the catalyst and the initial rate of polymerization. Shattering was shown to occur by the buildup of hydraulic forces within the pore structure of the silica at the beginning of the polymerization, and no further shattering was said to occur after the initial breakup of the carrier. BET and mercury porosimetry studies indicated that pores below ca. 30–100-nm diameter were not involved in the shattering process. Additional conclusions concerning the nature of the fragmentation process were later shown by the same author to be incorrect due to artifacts introduced in the high-temperature ashing process.[2]

Conner et al.[5] were able to trace changes in catalyst support structure back to the initial moments of the polymerization. Gas-phase polymerization of catalyst particles in the holder of a microbalance allowed very close control over the extent of polymerization within the range of 0–2 vol/vol (volumes of polymer per pore volume of carrier). Soxhlet extraction of the resulting polymer/catalyst particles followed by plasma ashing of the residual extracted particles below 200 °C removed most of the polymer from the pores of the carrier, leaving behind a tenuous skeleton of silica whose pore structure could be explored. Mercury porosimetry results at these low levels of polymerization did not differ from those obtained by MacDaniel at the higher levels of polymerization and so revealed that the shattering of the silica network was occurring even while the pores of the carrier were being filled with polymer for the first time. The porosimetry data were interpreted to mean that 50–100-nm-diameter fragments and larger were being formed, while the smaller pores within these larger fragments remained undisturbed.

As pointed out by Conner, mercury porosimetry is most suited for the measurement of collective properties of the pore structure in an entire sample and cannot discriminate between different events occurring in different locations within individual particles. Mercury porosimetry does not directly address the question of particle size or size distribution of residual support or its spatial distribution within the growing polymer particle, except to indicate a limiting lower particle size of ca. 50-nm diameter. Until noninvasive techniques[6] have been perfected, characterization via microscopic techniques appear to be required for a meaningful study of support effects.

II. Experimental Section

Samples. In order to make full use of the insights obtained in previous mercury porosimetry work, we conducted our scanning electron microscopy (SEM) studies of the initial fracturing process (0–2 vol/vol polymerization) using the same batch of catalyst and partially polymerized nascent polymers employed by Conner et al.[5] (Table I). Some of these samples were subsequently oxygen plasma ashed in our laboratory as reported below. We

0024-9297/92/2225-3910$03.00/0

Table I

series	sample	pore vol, cm^3/g	sample descripn
I	1	2.3	calcined (chromium oxide) silica catalyst
I	2	2.3	catalyst with polyethylene[a]
I	3	2.3	sample I-2 O_2 plasma-ashed at UM
II	1	1.7	catalyst with polyethylene[a]

[a] Catalyst meshed to 63–125-μm diameter, followed by a brief reaction at 100 °C at atmospheric pressure in ethylene/nitrogen (90/10), affording a product yield of 1.3 g/g of catalyst.

also examined the Davison 952 silica support by transmission electron microscopy (TEM) and SEM.

SEM–EDS–TEM. The major instruments employed were a JEOL JSM-35C scanning electron microscope, a Kevex 7000 energy dispersive (EDS) X-ray spectrometer retrofitted with a Quantum thin window detector which enables elements as light as fluorine to be readily detected, and an AEI 801 transmission electron microscope operated at 60 kV. Profiling of catalyst composition and catalyst concentration throughout the sectioned particle was achieved by obtaining relative Si, metal, and halide atomic intensities over a given 2 μm × 2 μm patch. Relative concentrations were obtained by normalizing on the silicon peak. Profiling was conducted by measuring changes in atomic composition from one patch to the next along a radial line of the sectioned particle.

Oxygen Plasma Ashing. A Tegal-Plasmod plasma asher (March Instrument Co., CA) was modified to enable a more accurate reading of the current in the radio-frequency power supply, which ranged from a threshold of 20 mA to a maximum of 100 mA. The modification entailed installing an ammeter readable to 1 mA in parallel with the meter supplied in the instrument. Since the plasma asher we employed is designed to nominally supply 100 W of radio-frequency power, we assumed a linear correlation to exist between the current reading and radio-frequency power: consequently, our experiments were all conducted at a nominal 25 W (25 mA) and 500 Torr oxygen pressure. The chamber was rough-pumped to less than 20 mbars and then back-filled with oxygen. Pressure was maintained by pumping continuously on the chamber in which oxygen was supplied through a leak valve. Since micrometer-sized fragments are generated in the plasma ashing, it is important to have a micrometer-sized particle filter installed in the backfilling vent line so as to avoid sample contamination from adventitious dust.

To minimize temperature buildup, the instrument was operated in a pulsed mode with a cycle of 10 min on and 10 min off. Maximum temperatures attained during plasma ashing were estimated by placing self-adhesive temperature recording labels (T-Dots, Cole-Parmer Instrument Co.) on a glass plate adjacent to the specimens during plasma ashing; ashing rates were kept low enough so that the highest temperature recorded was less than 60 °C. This precaution precluded alteration in the structure of the particle due to melting or sagging of the particle.

Ashing of untreated particles without Soxhlet extraction not only proved possible but probably led to a more faithful preservation of overall particle morphology, since the embedded inorganic components are perturbed less and since residual polymer can act as supporting lattice. Plasma ashing of the original support or catalyst particles did not lead to visible changes in the particle morphology. Plasma ashing of a partially polymerized catalyst particle preferentially removed the generated polymer and left behind a potentially highly friable residual structure. As demonstrated by Conner,[5a] plasma ashing should be halted when there is still a small amount of polymer present, even if full ashing is intended, to act as netting for the ashed particle and to keep air currents in the asher from blowing away micrometer-sized fragments during venting of the chamber.

Cryomicrotomy. A Reichert Ultracut-E microtome fitted with an FC-4 low-temperature sectioning system was operated with liquid-nitrogen gas cooling. Each sample was separately embedded in a thermosetting resin and cured overnight (>16 h) in a Beem capsule. Araldite M (a polyester) was used in the series I study (60 °C bake) and Buehler epoxy in series II at 22 °C (see Table I for sample/series description). The resin of choice is Buehler epoxy which cures overnight at room temperature. A dozen or so particles were placed in a 6-mm-diameter Beem capsule which was then filled with the epoxy formulation (five parts resin to one part hardener). The particles settled into the truncated pyramidal base. Air bubbles were removed from around the submersed particles by tapping the capsule or teasing them gently free with an orangewood stick. It bubbles are a problem, the liquid resin could be added to the particles under vacuum by means of a dropping funnel.

Optimal sectioning temperatures varied from sample to sample. Lower temperatures tended to give smoother cuts for polymer-rich samples. The sectioning temperatures were as follows:

	temp, °C		
sample	chamber	sample	knife
I-1,3	−10	10	20
I-2	−94	−50	−40
II-1	−95	−50	−40

The pyramidal stubs exposed by microtoming were glued to 2.5-cm-diameter carbon SEM plates with Du Pont Duco cement and grounded with conductive graphite paint. A thin layer of carbon was then vapor-deposited on the mounted samples to bleed off excess electron charge which would otherwise accumulate on insulating materials during normal SEM examination. This carbon was easily plasma-ashed away in studies requiring sequential ashing/examination, such as when proper etch times had to be established. Final plasma-ashed samples requiring high magnification were coated with an evaporated layer of gold to improve image quality at the higher magnifications.

Videotaped Polymerizations. Olefin polymerization catalysts were placed on the sample stage of an inert-gas microscopy cell equipped with inlet and outlet gas lines and a pressure glass window mounted into the screw-cap top of the cell. The entire cell and entry gas line were wrapped in heating tape. The polymerization temperature was monitored via a thermocouple buried in the tape jacket; runs were conducted from room temperature to 100 °C and from atmospheric pressure to 15 atm. Polymerizations were run under a Reichert Zetopan optical microscope using dark-field illumination or under an Olympus SZH-ILLD stereo zoom microscope. Runs are currently documented via a Javelin Chromachip II JE3462HR videocamera and a Mitsubishi BV-1000 super-VHS time-lapse recorder; data can also be saved in color or 256 gray scale on a Mac II computer equipped with a video grabber board.

Thermal Ashing of Polymer Particles. Ten grams of fully grown polymer particles were ashed at ca. 650 °C. The resulting ash was treated in an aqueous slurry in an ultrasonic cleaner for 30 min and examined by SEM. A wide variety of agglomerates were found which consisted of reaggregated submicrometer silica particles and unreacted silica particles.

III. Results and Discussion

Isolation and Immobilization of Silica Residues. The dimensional scale at which catalyst fragmentation occurs is readily accessible by SEM and associated techniques. Kakugo et al.[7] had studied the internal structure of cryomicrotomed nascent polypropylene particles by TEM. In contrast to their reported difficulties[7a] with $MgCl_2$-supported and unsupported $TiCl_3$ olefin polymerization catalysts, we found the silica-supported catalysts and nascent polymers highly suitable for SEM studies. However, special sample preparation procedures first had to be developed to overcome the problems cited by Kakugo. The fragmentation phenomena of interest occur underneath the exterior surface of the catalyst, which becomes obscured by the growing polymer immediately upon induction of polymerization. At moderate conversion, the fragmented silica is dispersed at higher and higher dilution within an ever-expanding polymer particle and thus is more and more difficult to detect. In the fully

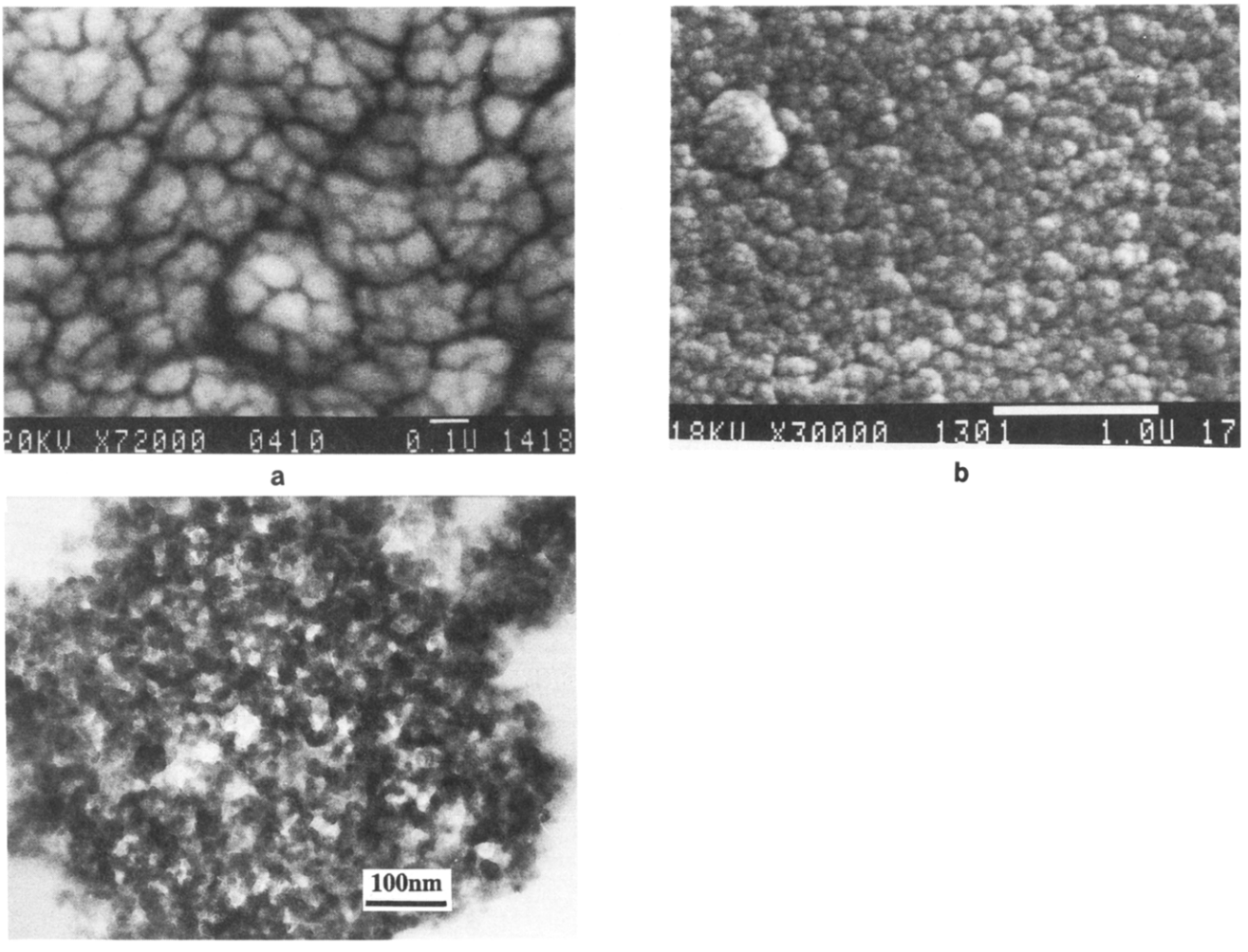

Figure 1. Davison 952 silica gel: (a) surface microstructure, SEM ×72 000; (b) internal microstructure exposed by microtomy of of the embedded particle, SEM ×30 000; (c) internal microstructure, microtomed thin section of an embedded particle, TEM ×160 000.

grown polymer particle, the support constitutes only 0.01–0.03 wt % of the polymer particle; extrusion of the polymer into film entombs the fragmented catalyst residues in a grave of molten polymer. At these different stages of particle growth and polymer workup, different techniques proved to be necessary to remove polymer, to stabilize the three-dimensional residual lattice, and to obtain access to the interior of the particle or to the interior of the extruded film.

At low conversions, we were able to expose the interior of the particles without obscuring or altering structural features by embedding particles in an inert matrix, followed by cryomicrotomy. At higher conversion, the original silica support is so finely divided that it is seldom possible to find residues within the embedded particle via the above techniques. Some information of still-disputed nature, however, is obtainable by full plasma-ashing of the particle. A cobwebbed metal oxide structure is left behind whose three-dimensional shape and texture mimic analogous features of the original polymer particle. Finally, special modifications of the plasma-ashing technique allowed us to isolate and characterize micrometer-sized inorganic residues in the blown film.

Structure of the Catalyst. Davison 952 has become a standard catalyst support for studies of olefin polymerizations.[2] The primary building blocks of the silica support are 10–50-nm-diameter spheroids formed during the polymerization of silicic acid solution and subsequent aggregation of colloidal silica. These are loosely cemented into larger aggregates which, in turn, are packed into even larger clusters. The channels between the primary particles as well as between the clusters are void pores. Specific structural properties of the support such as particle size, surface area, pore size, and pore-size distribution depend on the preparation procedures. These support properties influence the polymerization properties of the Cr-based olefin polymerization catalyst and control the morphology of the resulting polymer.

Parts a and b of Figure 1 are SEMs of the surface of Davison 952 silica gel at different magnifications. The surface is smooth and structureless on the macroscale, but at 1000× can be seen to consist of rounded nodular clusters of ca. 0.2–0.5-μm diameter which, in turn, can be seen at 72 000× (Figure 1a) to consist of nodular aggregates 0.05–0.1 μm in diameter. A similar morphology is observed in the interior by examining embedded/microtomed sections, except that the cluster size appears to be slightly smaller. The physical treatment of embedding and microtoming has not obscured or altered the physical structure of the exposed support. The power of the embedding/microtoming method can further be seen in the TEM image of a Davison 952 silica particle that was embedded, cured in epoxy, and microtomed into 100-nm sections. The presumably primary 10–50-nm particles as well as the pore structure are readily visible (Figure 1c).

Internal Structure of the Catalyst at Low Conversions. Kakugo et al.[7] had observed a pronounced nodular structure in nascent polypropylene obtained with

a $MgCl_2$-supported and unsupported $TiCl_3$ Ziegler catalyst, where the polymer replicates the microstructure of the metal halide crystallites. Our results with silica-supported chromium catalysts differ from the above on a fundamental level. After polymerization to give 1.3 g of polymer/g of catalyst (1 pore volume), cross-sectioned polymer/catalyst particles which have not been plasma-ashed show a smooth plane having a fine-textured granular structure rather than the nodular structure of the silica support or the nodular structure of the nascent polymer around $MgCl_2$ microparticles observed by Kakugo. The confining effect of the silica carrier first forces the polymer to fill available voids, generating a compact and compressed polymer unit rather than isolated nodular adducts.

The confining and templating effect of the carrier during the initial pore filling is also documented in the videotaped polymerizations. On initiation, silica-supported catalysts tend to take up ethylene without any evidence of changes in the size or shape of the catalyst particle. On continued polymerization, especially at elevated pressure, there is a one-time explosive growth of the particle followed by subsequent continuous slow growth until the end of the polymerization. The fully grown polymer particle has replicated the shape of the nascent particle after the initial explosion. In contrast, Ziegler catalysts not supported on silica gel showed an immediate slow growth in particle size. Replication of the nodular metal halide morphology occurred from the initial moments of the polymerization. These contrasting results fit the visualization of polymer filling the empty pores of the silica carrier, buildup of hydraulic pressure, rupture of the particle, and continued growth.

Microscopy polymerization also proved useful as a preparative tool. Close visual monitoring of the polymerization process allowed us to stop polymerization and obtain individual polymer particles at the current stage of growth. These specially grown particles could subsequently be examined by SEM and other characterization techniques.

Complete plasma ashing, partial plasma ashing, and plasma ashing of already embedded cross-sectioned particles can be conducted. Each of these treatments provides insights into different aspects of the polymerization process. The order of steps in the sample preparation sequence strongly influences the morphology of the resulting ashed particles. When low-conversion particles are plasma-ashed before embedding and microtoming, an expanded structure full of cracks is obtained (Figure 2a). However, when polymer/catalyst particles are first embedded and microtomed and then gently plasma-ashed, one obtains compact ashed particles with the morphology of the original unashed particles (Figure 2b).

Plasma ashing of the particles before embedding removes the stabilizing polymeric lattice and permits motion of the cracked silica lattice. Individual cracked components tend to separate from each other, so that the fragments can be analyzed and counted. We have found the sequence of ashing followed by embedding to be useful in studies of the pattern of support fragmentation and for monitoring fragmentation kinetics during the various stages of polymer growth as a function of various catalyst preparation and polymerization process parameters.

Plasma ashing of the particles after embedding and cross-sectioning provides more reliable information about the internal microstructure of the particle during the growth process. Plasma ashing is conducted in a surface plane on a molecular scale.[8] Therefore, first, any minor local expansion due to heat generated by the plasma cannot

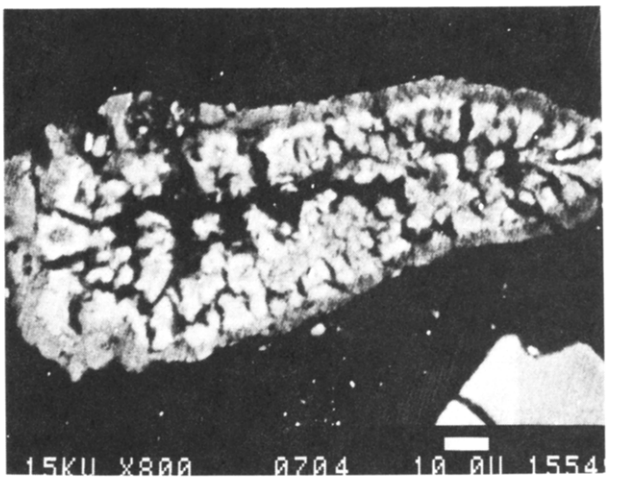

a

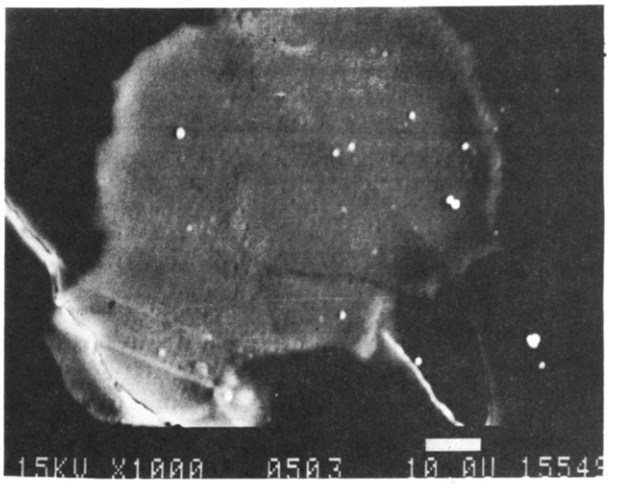

b

Figure 2. Polyethylene/catalyst particles (1 vol/vol): (a) O_2 plasma-ashed and then embedded and cryosectioned, SEM ×800; (b) embedded, cryosectioned, and then O_2 plasma-ashed, SEM, ×1000.

be relieved by motion of the particle within the plane. Second, the amount of internal thermal expansion is minimal at temperatures below 60 °C because the underlying embedding medium acts as a heat sink and helps prevent softening or melting of the exposed surface. Third, plasma ashing is confined to the two-dimensional plane of the exposed surface, and undercutting by the plasma is minimal. Sequential layers of material can therefore be removed between SEM observations. Finally, the embedding medium acts as a structural support for the particle, immobilizes the fragmented inorganic components, and thereby prevents the collapse of the particle while the original polymer lattice is gradually etched away.

Studies on thermally ashed materials confirmed that high-temperature ashing caused unacceptable rearrangement, cracking, and fusing of the residual silica network. But even though it is a gentler technique, plasma ashing still has to be conducted carefully. Plasma ashing conducted without temperature monitoring may lead to nonreproducible results due to the potential melting and sagging of particles. Even low-temperature plasma ashing may lead to misleading conclusions if the particle is allowed to fall apart. We suggest that measurements of pore diameters of plasma-ashed samples need to be interpreted with caution, regardless of whether measured via mercury porosimetry or microscopy. If pore diameters within the residues of the support are shown to be larger

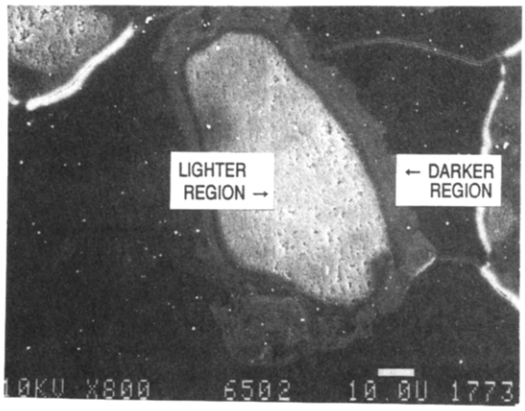

A

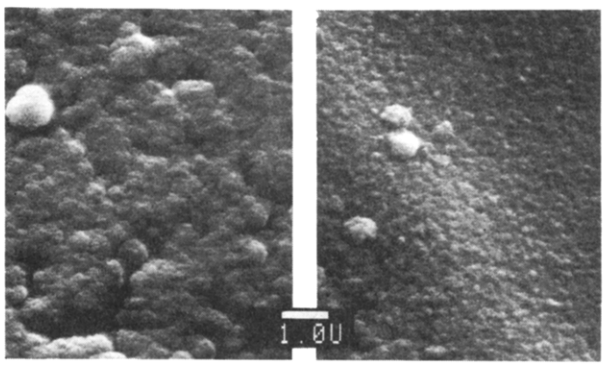

B C

Figure 3. Polyethylene/catalyst particle (1 vol/vol): (A) cryosectioned after embedding, SEM ×800; (B) lighter region enlarged, SEM ×10 000; (C) darker region of the particle enlarged, SEM ×10 000.

after polymerization, cracking of the support undoubtedly has taken place on the dimensional scale indicated by mercury porosimetry. The observed quantitative increase in pore diameter should however be taken as a maximal value, since expansion of unembedded particles during plasma ashing is a strong possibility. Our SEM studies have consistently revealed wider channels in the residual silica lattice for samples which had not been embedded before plasma ashing.

Initiation of Polymer Formation. The initiation of polymerization lead to a buildup of hydraulic pressure within the catalyst particle, which in turn may lead to unanticipated structural changes within the particle. Sufficiently severe structural changes may become replicated in the morphology of the polymer particle, so that the desired direct replication of support morphology into polymer morphology is not obtained. Control over the interior and exterior structure of the polymer/catalyst particle in the early moments of the polymerization is therefore of critical importance. Our techniques enabled us to monitor this interior structure of the nascent polymer. Particles of sample II-1, a Davison 952-based Cr catalyst polymerized by Conner et al.[4] to barely fill all pores (1 vol/vol) and studied closely via mercury porosimetry by that group, was selected for a detailed autopsy. Embedded, cryomicrotomed samples were examined before and after subsequent plasma ashing. In general, it proved difficult to distinguish the morphology of the polymeric component from that of the silica component in scanning electron micrographs of unashed samples, since both feature a similar microgranular morphology. A significant difference in brightness in various regions of many cross-sectioned particles was observed (Figure 3A). EDS indicated that the sectioned surface was predominantly carbonaceous in both the light and the dark regions of the sectioned plane but that the lighter regions were comparatively richer in silicon. The surface thus consists of a conformal coating of polymer growing from within siliceous material; dark regions represent areas where polymer growth has progressed to a greater degree than in the lighter areas. It is interesting to note that polymerization had not proceeded uniformly throughout the particle, even though enough polymer had been made to nominally fill all pores with polymer.

With the identification of the microtome-exposed interior surface as consisting predominantly of polymeric material, SEM micrographs can readily be interpreted in terms of replication of the silica structure by the polymer. The lighter regions (Figure 3B) consist of overgrown nodules of polymer shaped in the form of the underlying silica nodules, where the polymeric nodules have just begun to grow together. The darker regions (Figure 3C) consist of already more fully merged nodular growths, which in denser regions have undergone further growth to give an almost featureless plane of polymeric material.

Plasma ashing of the sectioned particles removed the carbonaceous material to a depth > 3 μm and restored the underlying silica surface (Figure 4), as shown by the drastic change in appearance of the sample and the dominance of the silicon peak in the EDS scan of the new surface. The morphology of this ashed cross section strongly resembles the corresponding morphology in the original catalyst, except that the agglomerated nodules have apparently increased in size, and the subcomponents of these nodular aggregates can be more readily distinguished visually than in the cross section of the original catalyst. The increase in the nodular dimensions appears to be greater in the lighter (less polymerized) regions of the particle.

The above observations suggest that polymer is formed within the 0.2–0.5-μm nodules, which stretch and expand to about double their size. The subcomponent 0.05–0.1-μm nodules become more separated from each other due to the stretching and expansion of the parent nodule, but themselves do not appear to have been crushed, pulled apart, or otherwise destroyed on polymer formation. In the regions of sparse polymer growth, nodules are still able to expand freely because there is little interference or hydraulic pressure from their neighbors. In the areas of the particle where polymer growth has progressed further, polymerizing and growing nodules come into contact with polymers from neighboring nodules, leading to merged assemblies of polymers as the increasing pressure pushes the nodules together. Further polymerization results in a nearly featureless mass of compressed polymer, which eventually will give rise to a voids-free, filled polymer particle.

The basic morphological unit of polymer growth appears to be the 0.2–0.5-μm clusters of SiO_2 seen in the original catalyst substrate particles and not the smaller structural entities of the polymerization-active transition-metal complexes. We were not able to distinguish residual silica morphologies in polymers derived from chemisorbed chromium catalysts versus residues derived from silica-impregnated $MgCl_2/TiCl_4$ catalysts. The silica support thus appears to usurp the role of the basic template of growth from the transition-metal compound or from the $MgCl_2$ crystallites, respectively.

Internal Structure of Carrier at Higher Conversions. Embedded and cross-sectioned nascent polymer particles at 5–100 vol/vol conversion were examined mainly by SEM–EDS Si mapping. In continuation of the breakup of the silica structures, the Si EDS maps generally

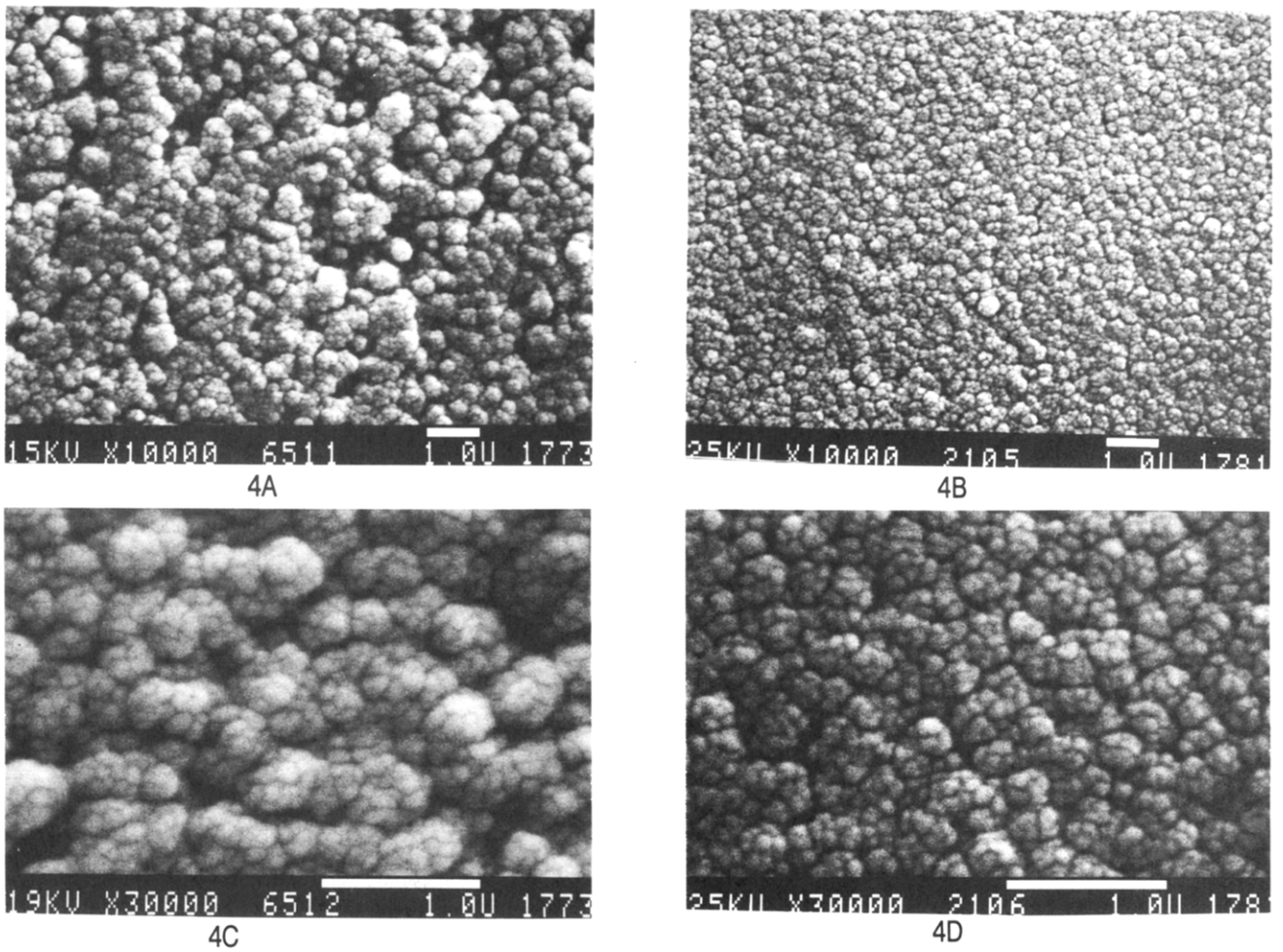

Figure 4. Cryosectioned particle in Figure 3 O_2 plasma-ashed to remove surface polymer: (A) lighter region, SEM ×10 000; (B) darker region near the edge of the particle, SEM ×10 000; (C) enlargement of (A), ×30 000; (D) enlargement of (B), SEM ×30 000.

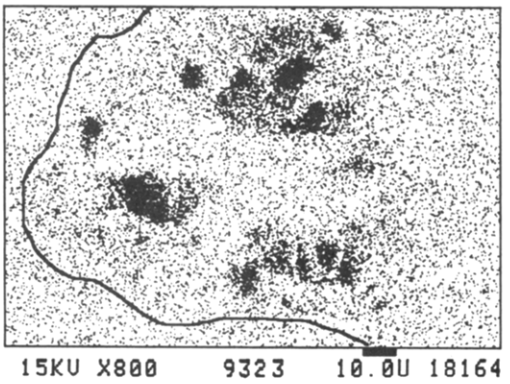

Figure 5. Reverse video EDS silicon distribution map, ×800. Polyethylene/catalyst particle (5 vol/vol), embedded and then cross-sectioned. Region outlined comprises approximately half the particle cross section.

became more and more diffuse as the amount of polymer per particle increased. For some particles, the Si distribution map was uniform, indicating a uniform extent of polymerization within the particle. However, a large fraction of particles exhibited individual islands of silica-rich material, indicating continuing nonuniform polymerization within the particle (Figure 5). These residual islands of higher Si concentration often occurred off-center or even near the periphery of the particles. However, the islands tended to become more diffuse and fewer in number at higher levels of polymerization within the 5–100 vol/vol range, indicating that less reactive regions eventually also formed polymer. For Ziegler catalysts, we were able to correlate regions of high polymer growth with regions of high catalyst concentration within the particle via EDS profiling of catalyst particles.

Internal Structure of Fully Polymerized Particles. At conversions above ca. 100 volumes of polymer/pore volume of catalyst, Si mapping of the embedded cross-sectioned particles no longer gave useful results due to excessive dilution of the support within the growing polymer particle. Isolated islands of higher Si concentration could no longer be found. However, almost complete plasma ashing of particles at temperatures far below the softening point of the polymer uncovered the residual support in a new arrangement. A tenuous webbing of silica is obtained for Cr-based catalysts,[9] while Al/Si webbings are observed for Ziegler-based polymer particles (Figure 6). These three-dimensional cobweb structures replicate the initial morphology of the polymer particle in appreciably shrunken form. The webbings are composed of metal oxide beaded strands of 1-μm diameter or smaller, and as a rule do not contain any larger fragments. We interpret these structures to be reagglomerations of dispersed, submicrometer size silica or alumina/silica microparticles which deposited on the exterior surface of the shrinking polymer particle during plasma ashing. We believe that the largest chunks of material seen within the cobweb represent the upper size limit of the residual support structure at the end of the polymerization process.

Solid Residues in Extruded Films. Under commercial conditions, polymer particles grow to about 3000–10 000 volumes of polymer/volume of catalyst, and silica residues can no longer be seen in individual particles. The

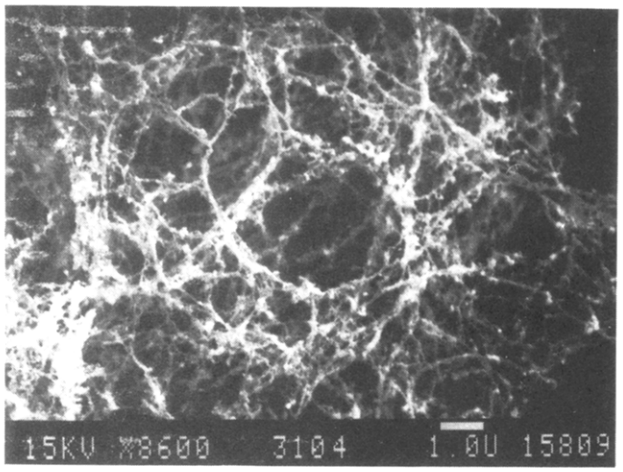

Figure 6. Closeup of an inorganic web remaining after the organic phase of a polymer particle (conversion >1000 vol/vol) has been totally removed by O_2 plasma ashing for 16 h, SEM ×8600.

average properties of the residual support can nevertheless be studied indirectly by examining the inorganic residues in an extruded film. Gentle plasma ashing of an extruded film exposes the inorganic residues embedded within and on the surface of the film. Plasma ashing of a ~50-μm film was continued down to a film thickness of a few micrometers without appreciable loss of residual particles, as demonstrated by sequential monitoring of samples during the ashing process. SEM and EDS studies of the ashed film allowed identification of the chemical composition and morphological features of the residues. Except for some occasional unfractured catalyst particles, catalyst-derived inorganic residues larger than 1 μm were conspicuous by their absence. In contrast, solid additives and inorganic contaminants of dimensions on the order of 1 μm and larger (antiblock agents, etc.) could be readily seen and their composition determined.

Other Techniques. The described methods of plasma ashing, embedding, and cross sectioning allow subsequent study of the silica fragmentation process by a variety of surface analysis techniques, of which only SEM and EDS have been described herein. Characterization of molecular-level phenomena occurring in the interior of catalyst precursors and nascent polymers has also proven feasible using techniques such as DRIFT, infrared microscopy, ESCA, and SIMS.

The changing structure of the silica support, its role during the various stages of the polymerization, and its final fate within the polymer particle and an extruded film has been elucidated for chromium-based olefin polymerization catalysts by these techniques. Analogous experiments with silica-supported Ziegler–Natta catalysts gave parallel results.[10] Descriptions of polymer growth processes made possible by application of these characterization tools have been provided elsewhere.[10c]

Acknowledgment. We acknowledge helpful discussions as well as receipt of samples from Profs. Wm. C. Conner, Jr., and R. L. Laurence, University of Massachusetts.

References and Notes

(1) Hogan, J. P.; Banks, R. L. U.S. Patent 2,825,721, March 4, 1958.
(2) (a) McDaniel, M. P. *Adv. Catal.* **1985**, *33*, 47. (b) Marsden, C. E. *Preparation of Catalysts. V*; Poncelet, G.; Jacobs, P. A., Grange, P., Delmon, B., Ed.; Elsevier Science Publishers B. V.: Amsterdam, 1991.
(3) Karol, F. J.; Karapinka, G. L.; Wu, C.; Dow, A. W.; Johnson, R. N.; Carrick, W. L. *J. Polym. Sci., Polym. Chem. Ed.* **1972**, *10*, 2621.
(4) McDaniel, M. P. *J. Polym. Sci., Polym. Chem. Polym. Chem. Ed.* **1981**, *19*, 1967.
(5) (a) Weist, E. L.; Ali, A. H.; Naik, B. G.; Conner, Wm. C. *Macromolecules* **1989**, *22*, 3244. (b) Conner, W. C., private communication.
(6) Conner, W. C.; Webb, S. W.; Spanne, P.; Jones, K. W. *Macromolecules* **1990**, *23*, 4742.
(7) (a) Kakugo, M.; Sadatoshi, H.; Yokoyama, M.; Kojima, K. *Macromolecules* **1989**, *22*, 547. (b) Kakugo, M.; Sadatoshi, H.; Sakai, J.; Yokoyama, M. *Macromolecules* **1989**, *22*, 3172.
(8) Dilks, A.; VanLaeken, A. In *Physicochemical Aspects of Polymer Surfaces*; Mittal, K. L., Ed.; Plenum Press: New York, 1983; Vol. 2, p 750.
(9) Plasma-ashing studies of fully grown polymer particles at Union Carbide were initiated by Dr. W. von Dohlen (dec).
(10) (a) Karol, F. J.; Wagner, B. E.; Levine, I. J.; Goeke, G. L.; Noshay, A. In *Advances in Polyolefins*; Seymour, R. B., Cheng, T., Eds.; Plenum Publishing Corp.: New York, **1987**; p 337. (b) Wagner, B. E.; Niegisch, W. D. *Proc. Am. Chem. Soc., Div. Polym. Mater.: Sci. Eng.* **1991**, *64*, 139. (c) Wagner, B. E.; Karol, F. J. Conference Proceedings, 6th International Conference on Polyolefins, Society of Plastics Engineers, RETEC, Feb 1989, Houston, TX, p 77.

Registry No. Davidson 952, 7631-86-9; polyethylene (homopolymer), 9002-88-4.